System Modelling of an Electric Two-Wheeled Vehicle for Energy Management Optimization Study

Sawant, Swapnil
School of Mechanical, Aerospace and Automotive, Coventry University

Raja Mazuir Raja Ahsan Shah
School of Mechanical, Aerospace and Automotive, Coventry University

Rahman, Mostafiz
School of Mechanical, Aerospace and Automotive, Coventry University

Abd Rashid Abd Aziz
Instititute of Transport Infrastructure, Universiti Teknologi Petronas

他

https://doi.org/10.5109/4491656

出版情報：Evergreen. 8 (3), pp.642-650, 2021-09. 九州大学グリーンテクノロジー研究教育センター
バージョン：

System Modelling of an Electric Two-Wheeled Vehicle for Energy Management Optimization Study

Swapnil Sawant[1], Raja Mazuir Raja Ahsan Shah[1]*, Mostafiz Rahman[1], Abd Rashid Abd Aziz[2], Steve Smith[3], Aidah Jumahat[4]

[1]School of Mechanical, Aerospace and Automotive, Coventry University, Coventry, United Kingdom

[2]Instititute of Transport Infrastructure, Universiti Teknologi Petronas, Seri Iskandar, Malaysia

[3]Veitis Limited, Maidstone, Kent, United Kingdom

[4]Faculty of Mechanical Engineering, Universiti Teknologi Mara, Shah Alam, Malaysia

*Author to whom correspondence should be addressed:
E-mail: mazuirra@yahoo.co.uk

(Received January 7, 2021; Revised September 6, 2021; accepted September 6, 2021).

Abstract: This study investigated the performance behaviour and energy management control strategies of an electrified two-wheeled vehicle (E-TWV). The power and energy demands were calculated through a high-fidelity E-TWV model. A lithium-ion battery (LIB) pack was designed and characterized according to electric motor power requirements. Three transient duty cycles, modified assessment and reliability of transport emission models and inventory systems (ARTEMIS), federal test procedure (FTP)-75, and world harmonized test protocol (WLTP) class 2 were used to assess the energy management control strategies. The E-TWV model has managed to meet the power demand with less than 2% across the speed range. The electric motor architecture demonstrated an improvement in the performance acceleration of the vehicle (pass-by accelerations = 4.5 s) and the energy consumption in all transient duty cycles via control strategies implementation and regenerative braking (< 60 W·h/km). All results were also validated using three energy sources, namely coal, natural gas, and combined (CC) gas turbine to determine the well-to-wheel carbon dioxide (CO_2) emission. The CC gas turbine produced 45 % less CO_2 g/km compared to coal which indicated that the E-TWV can only be successful if the source of energy to charge the LIB is clean and sustainable.

Keywords: electrification, powertrain, energy management, system modelling, driveability

1. Introduction

Carbon dioxide (CO_2) reduction is imperative due to climate change and global warming. The transportation sector is responsible for 25 % of global CO_2 emissions, according to the recent International Energy Agency report[1)]. Several action plans have been implemented to reduce the CO_2 emissions in the transportation sector such as a heat recovery technology in a fuel cell system[2)], and vehicle electrification is prominent among them. Deloitte Insights[3)] forecasted the passenger-car and light-duty vehicle sales in 2025 will reach 90 million units of which 11% is electric vehicles (EVs). In terms of two-wheeled vehicles, MotorCycles Data[4)] forecasted 69.9 million sales volume in 2025. Therefore, the compound annual growth rate of electric two-wheeled vehicle (E-TWV) between 2019 and 2025 is 10.35 %[5)]. Some countries plan to completely phase out the fossil fuel-based two-wheeled vehicle from 2025 such as India[6)], which has the biggest market for such vehicles. These policies are accelerating the E-TWV development in terms of the range anxiety associated with the battery energy density[7)], the cost premium that customer willing to invest for the product value[8)] and the charging infrastructure readiness to meet the high demand and fast charging requirement[9)]. The majority of E-TWV developers focuses on the effort to reduce the range anxiety issue and to minimize the cost premium for increasing the product demand[10)].

The system modelling technique is one of the popular approaches that can reduce the development time and cost, the project risks, and the chance of building several prototype vehicles. The system modelling based on multiphysics interactions can be used to analyze each of the vehicle sub-systems responses[11)]. For instance, Ali and Chakraborty[12)] implemented mathematical modelling to study the relationship between a thermal system and an energy system to improve vehicle fuel consumption. For two-wheeled vehicle application, transient power demands are required to represent the real-world road duty cycle that can be implemented for validation of the energy

management of the vehicle. One example is that Hanifah et al.[13] built and combined a mathematical chassis dynamic of the E-TWV model with an object-oriented model for energy management investigation based on new and obsolete test protocol, namely world harmonized test protocol (WLTP) and new European driving cycle (NEDC). To achieve the maximum range, it is important to identify the behaviour of the electric motor and drivetrain in the transient-state. It helps in optimizing the operating conditions in terms of power requirement and system efficiency. A study by Nguyen et al.[14] focused on the hybrid E-TWV control strategies a transient power demand for the energy management between rear-wheel internal combustion engine propulsion and front in-wheel motor. On the other hand, Chen et al.[15] used a combination of inverse and power mode switching control for efficiency improvement in hybrid E-TWV architecture based on a standard steady-state test protocol, ECE-R40 for a two-wheeled vehicle. To meet the performance attribute of E-TWV, there are several aspects of the design that need detailed consideration. For instance, the sizing of the electric motor has to take into account power demand at standing start and maximum steady-state conditions[16]. The driveability of E-TWV as a result of the electric motor characteristics must also be included in the design requirement. The driveability behaviour can be validated using the multiphysics model based on the standard automotive tip-in/tip-out event[17]. In terms of tailpipe CO_2 emissions, a fossil-fueled TWV produces an average of 110 g/km^{-1} [18].

This study solely focused on a high-fidelity fore-aft model development of high-performance E-TWV, and evaluate its characteristics in terms of sub-system/system efficiencies for well-to-wheel CO_2 reduction, as well as responses to the power demands. The performance and driveability characteristics of the E-TWV is also studied using maximum steady-state power demand and tip-in/tip-out event at 75 % wide open throttle respectively. The E-TWV model used a combination of transient power demands to represent a real-world application for the energy management study such as assessment and reliability of transport emission models and inventory systems (ARTEMIS), federal test procedure (FTP)-75 and WLTP class 2. The study also emphasizes the E-TWV model real-time simulation for control strategies development and system tuning capability.

2. Simulation approach for E-TWV

A multiphysics modelling method was used to examine the characteristics of the sub-system/system components under different power demands. The system architecture of the model was based on the existing rear-wheel drive (RWD) E-TWV with an electric motor connected to a rear-wheel via a chain-drive. The specifications of E-TWV is shown in Table 1.

Table 1. E-TWV specifications

Parameters	**Value**
Electric motor continuous power (kW)	16.0
Electric motor continuous torque (N m)	60.0
Vehicle weight (kg)	250.0
Operating voltage (V)	80.0
Battery capacity (kW h)	8.0
Drivetrain architecture	RWD
Chain-drive ratio	1.0:4.028
Frontal area (m^2)	0.5
Drag coefficient (including rider)	1.1
Front-wheel diameter (mm)	457.2
Rear-wheel diameter (mm)	457.2

The power demand of the E-TWV is calculated using Eq. 1

$$P_v = \left(\left(\frac{1}{2}\rho A C_d v^2 \right) + mg\, C_{rr} + ma + mg\sin\theta \right) v \quad (1)$$

The tyre rolling resistance is derived from the nonlinear tyre model properties based on Magic Formula[19]. The gradeability of the road can be neglected since the standard test procedures for all road duty cycles are based on a rolling road to mimic a flat road surface.

And the energy consumption is given by Eq. 2

$$\varepsilon = \int_0^t P_v \, dt \quad (2)$$

The battery direct current (DC) power is defined in Eq. 3

$$P_{dc} = V_o I_o \quad (3)$$

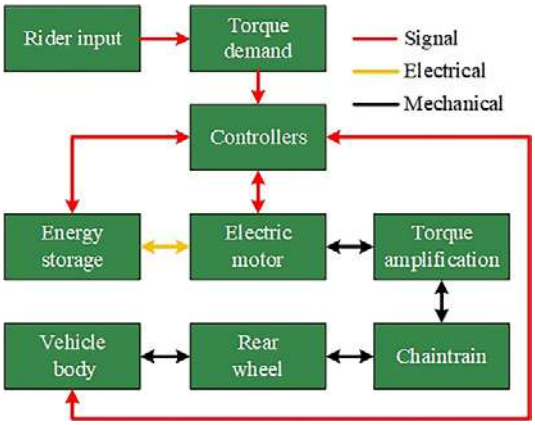

Fig. 1: E-TWV sub-system/system components interaction concept

Fig. 1 shows the conceptual architecture of E-TWV for the sub-system/system components interaction. The architecture of the E-TWV model comprised of powertrain subsystem, chassis subsystem, energy storage subsystem, controllers and driver model. The torque demand from the rider was fed to the controllers to optimize the level of interaction between the energy storage and the electric motor. The torque produced by the electric motor was amplified in the transmission and then transferred to the rear wheel via chain drive. The rear wheel and the vehicle body was connected by mechanical couplers. The rear wheel developed the tractive effort based on a non-linear tyre model as a function of vertical weight transfer between the front and rear wheels when the vehicle was in motion. The vehicle provided feedback to the controllers in terms of vehicle speed for power optimization.

From the conceptual architecture, the E-TWV model was built to capture the electrical and mechanical system interactions. Fig. 2 demonstrates the high-level system model architecture of E-TWV. The system model consists of Lithium-Ion battery (LIB) energy storage based on 21700 cylindrical LiNiMnCo (NMC) with 20 series (S) 28 parallel (P) cell arrangement. The cell maximum voltage is 4.2 V and the cut-off voltage is 2.5 V. The maximum continuous C-rate of the LIB cell is 2.0 C (10 amps). NMC battery has a good cycle life performance, which is one of the important requirements for EVs, compared to other types of chemistry such as NaMeO2 battery[20]. However, the NMC cost is considerably high. According to Xie et al.[21], another potential chemistry is Na-Ion based (Na3MPO4CO3) but required further development in EVs application.

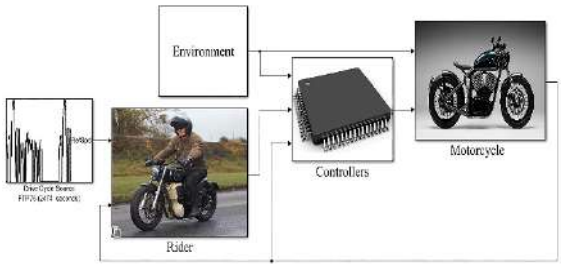

Fig. 2: A high-level multiphysics system model of E-TWV

The electric motor was based on the multi-inputs multi-outputs lookup table to represent the electric motor map. The outputs were an output torque and a LIB current as a function of LIB voltage, motor speed and torque demand. The electric motor performance characteristic is shown in Fig. 3. For the tractive effort input, the vehicle weight transfer was controlled by the vehicle centre of gravity (CoG) and the front and rear suspension compliances. The weight transfer is given by Eq. 4.

$$\Delta m = m\varphi \frac{h}{l} \qquad (4)$$

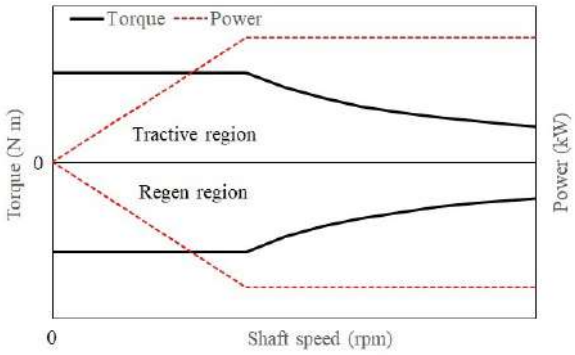

Fig. 3: Electric motor performance characteristic for tractive and regenerative efforts

In terms of the driver inputs, there were two types of test used in the system model to characterize the E-TWV, namely performance test and energy consumption test as shown in Fig. 4. For the performance test, the test schedule is shown in Table 2.

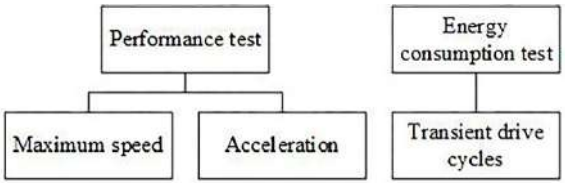

Fig. 4: Simulation test procedures of e-TWV

Table 2. Performance test schedule of E-TWV

Test procedures	**Methods**	**Rationale**
Maximum speed	Apply 100 % ramp power demand within	To evaluate the maximum speed

	0.5 seconds (s)	of E-TWV specifications
Acceleration	Apply 75 % ramp power demand within 0.5 s based on speed demands below 0 – 100 km h^{-1} 30 – 50 km h^{-1} 40 – 60 km h^{-1} 50 – 70 km h^{-1}	To simulate the performance of the E-TWV in terms of acceleration, overtaking and driveability

For the energy consumption test, three transient road duty cycles were used to reflect the real-world driving scenario as shown in Table 3. All of the road duty cycles represented the product profile of E-TWV in terms of the accelerations, power responses, and energy demands.

Table 3. Transient power demand profiles using standard road duty cycles

Parameters	**Modified ARTEMIS**	**FTP-75**	**WLTP class 2**
No. of phases (speed profile)	Urban cycle ½ Rural road cycle	Cold start Stabilized Hot start	Low Medium High
Maximum speed (km h^{-1})	83.8	91.2	85.2

To calculate the well-to-wheel CO_2 emission, the consideration of production, transmission and charging losses are taken into account using Eq. 5 below.

$$K_e = (U_e + T_e + C_e)\mathcal{E}_{km} \quad (4)$$

The charging losses are considered at 10 amps for home charging mode 2 standard[22]. Fig. 5 shows the transient speed profile as the input for the rider. For modified ARTEMIS, only the phases below 100 km h^{-1} are considered due to the maximum speed capability of E-TWV.

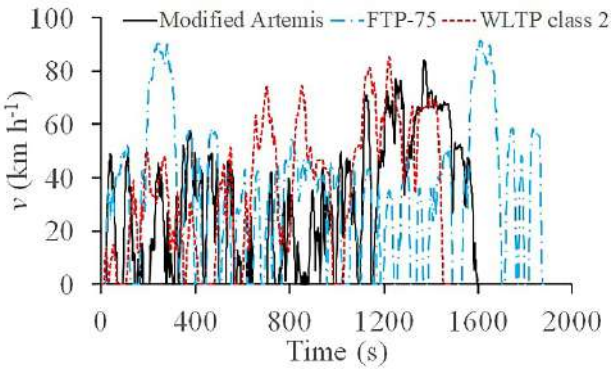

Fig. 5: Three standard road duty cycles based on transient power demands

3. Simulation test results

Based on the performance test procedures, the performance attributes of e-TWV is shown in Table 4. E-TWV is capable to achieve 110 km h^{-1}, which is a similar performance to most 125 litre fossil-fuel TWV. The pass-by acceleration in all speed ranges shows that the electric motor can operate at the same torque region and provided a good driveability attribute.

Table 4. Performance attributes of E-TWV

Test Parameter (km h^{-1})	**Results**
Maximum speed	110 km h^{-1}
Standing-start acceleration, 0 – 100	8.4 s
Pass-by acceleration, 30 – 50	4.5 s
Pass-by acceleration, 40 – 60	4.5 s
Pass-by acceleration, 50 – 70	4.5 s

Three results of transient road duty cycle tests covered the vehicle speed correlations, the LIB state of charge (SOC), the DC LIB power, the electric motor power and the LIB pack current. From the simulation results, the E-TWV model shows a good correlation in terms of vehicle speed in all road duty cycles as shown in Fig. 6 (a), Fig. 7 (a) and Fig. 8 (a). To achieve the desired vehicle speeds, sufficient electric motor power outputs were supplied to the rear-wheel for providing the tractive effort. Therefore, the controllers' block in the model ensured that the LIB energy storage provided adequate DC power levels to the electric motor.

During the operation of the E-TWV model on the road duty cycles, the current was continuously discharged and charged from the LIB energy storage. The amount of current discharged and charged was governed by the number of LIB cells in a series arrangement and directly proportional to the torque produced by the electric motor. The higher current discharged rate can cause a sharp drop in LIB SOC.

In the modified ARTEMIS road duty cycle as shown in Fig. 6, the E-TWV was able to achieve the maximum vehicle speed demand at 83.8 km h^{-1} with less than 1 % error across the cycle time. The complete cycle time for the modified ARTEMIS is 1600 s. The average and the maximum electric motor power demands in the urban cycle were 0.9 kW and 8.3 kW respectively. The trend of the electric motor power demand in the urban cycle was moderate and depleted 2.2 % of LIB SOC. On the other hand, in the rural road cycle, the average and the maximum electric motor power demands were 2.7 kW and 13.1 kW respectively. The high-speed demand caused LIB SOC to deplete 4.2 %. The average efficiency between the LIB and the electric motor in the modified Artemis was 13% (12.3 % in the urban cycle and 14.7 % in the rural road cycle), which are common due to the inverter efficiency between 80 % and 90 %. The LIB C-rate operated below the maximum threshold with 2.0 C at the urban cycle and 6.1 C at the rural urban cycle. The total range for the E-TWV at the modified ARTEMIS road duty cycle per single charge was simulated at 182.7 km.

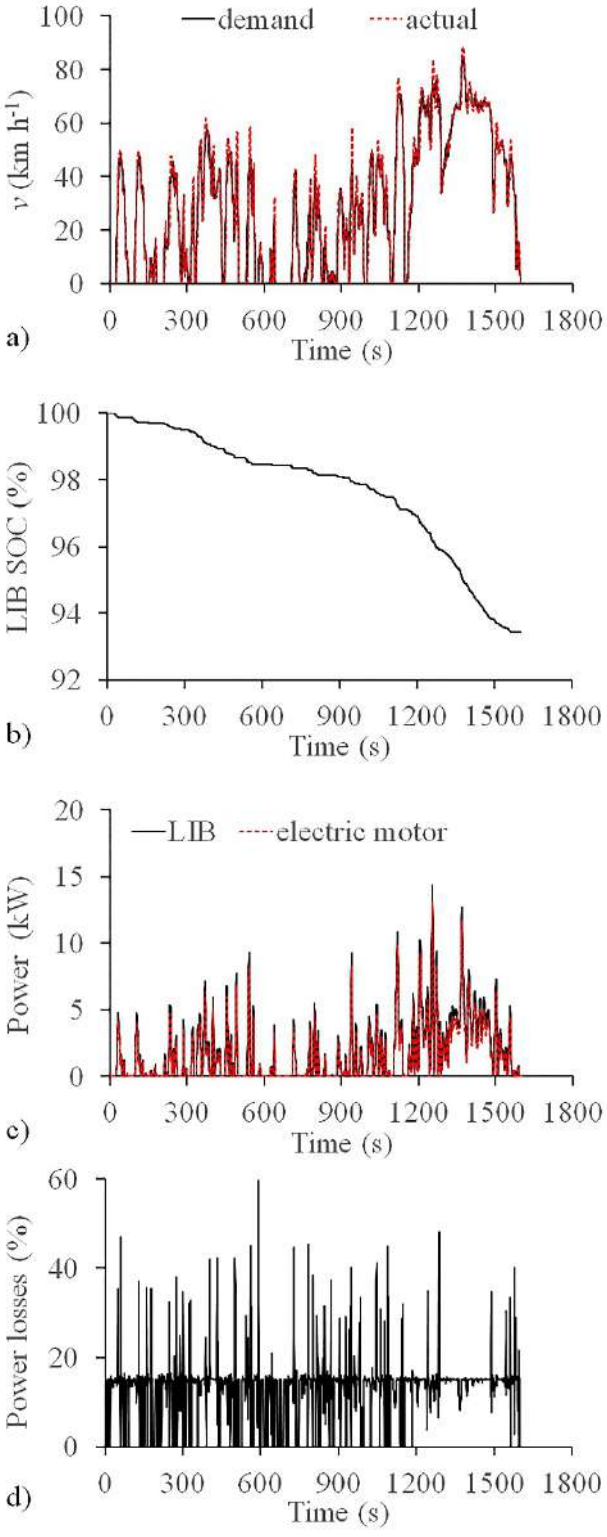

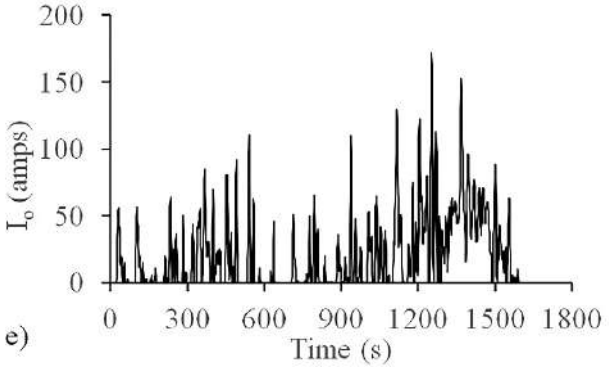

Fig. 6: E-TWV characteristic based on the modified ARTEMIS road duty cycle a) vehicle speed b) LIB SOC c) electrical power output d) electrical power losses and e) LIB pack current

For the FTP-75 road duty cycle (Fig. 7), the maximum vehicle speed demand at 91.2 km h^{-1} has been attained with less than 2 % error across the cycle time. The cold start cycle time is 1874 s and the hot start cycle time is 505 s. The average and the maximum electric motor power demands in the cold start cycle were 1.1 kW and 10.5 kW respectively. The higher electric motor power demand depleted the LIB SOC at a faster rate. No change of maximum electric power demand in the hot cycle except the average of 2.2 kW with a steep LIB SOC drop. The average efficiencies between the LIB and the electric motor in both cycles were similar at 13 %. As the electric motor power demand was less aggressive compared to the modified Artemis, the LIB C-rate required a maximum value of 6.0 C in both cycles. The total range for the E-TWV at the FTP-75 road duty cycle per single charge was simulated at 173.2 km.

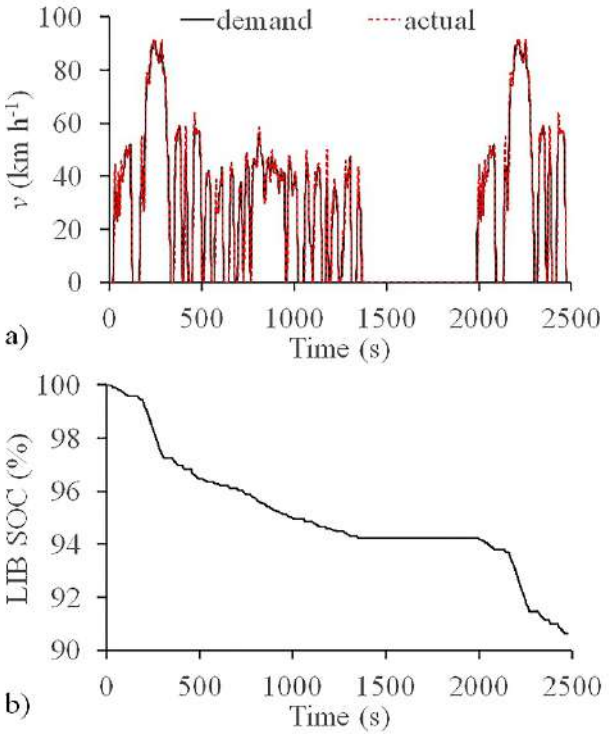

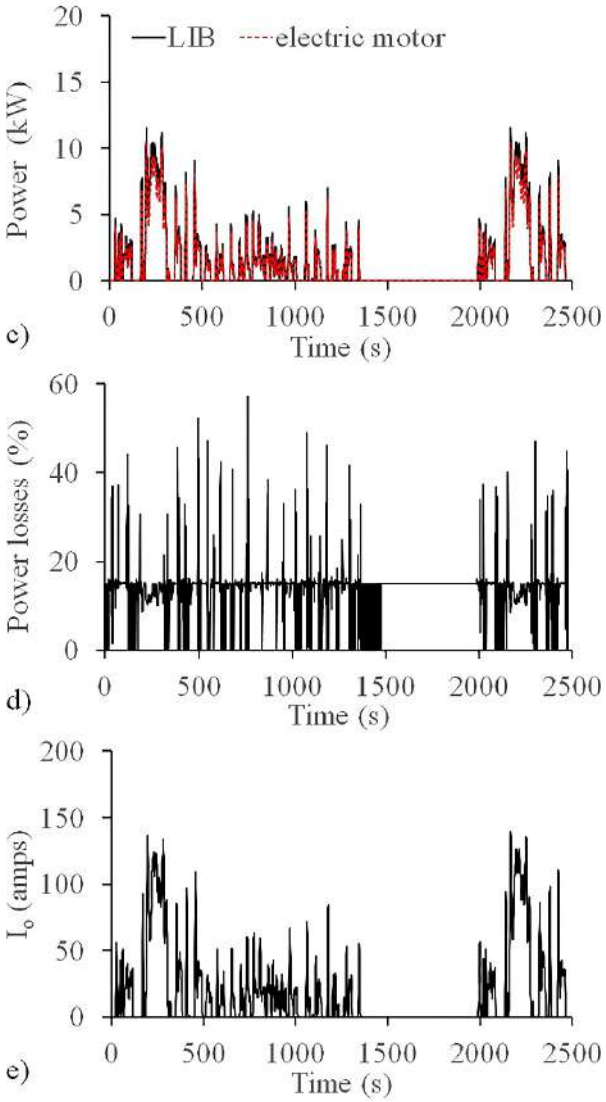

Fig. 7: E-TWV characteristic based on the FTP-75 road duty cycle a) vehicle speed b) LIB SOC c) electrical power output d) electrical power losses and e) LIB pack current

Similarly in the WLTP class 2 road duty cycle, the E-TWV met the maximum vehicle speed demand at 85.2 km h^{-1} with less than 2 % error across the cycle time of 1477 s as shown in Fig. 8. The respective average and maximum electric motor power demands in the low cycle were 0.54 kW and 3.8 kW, in the medium cycle were 1.6 kW and 6.1 kW, and in the high cycle were 2.7 kW and 9.1 kW. In the cold cycle, the LIB SOC depleted steadily and at higher rates in the medium and high cycles. The average losses in all cycles were between 13.4 % and 13.9 %. In terms of LIB C-rate, the lowest and maximum values are 1.9 C and 4.3 C respectively. The total range for the E-TWV at the WLTP class 2 road duty cycle per single charge was simulated at 194.1 km.

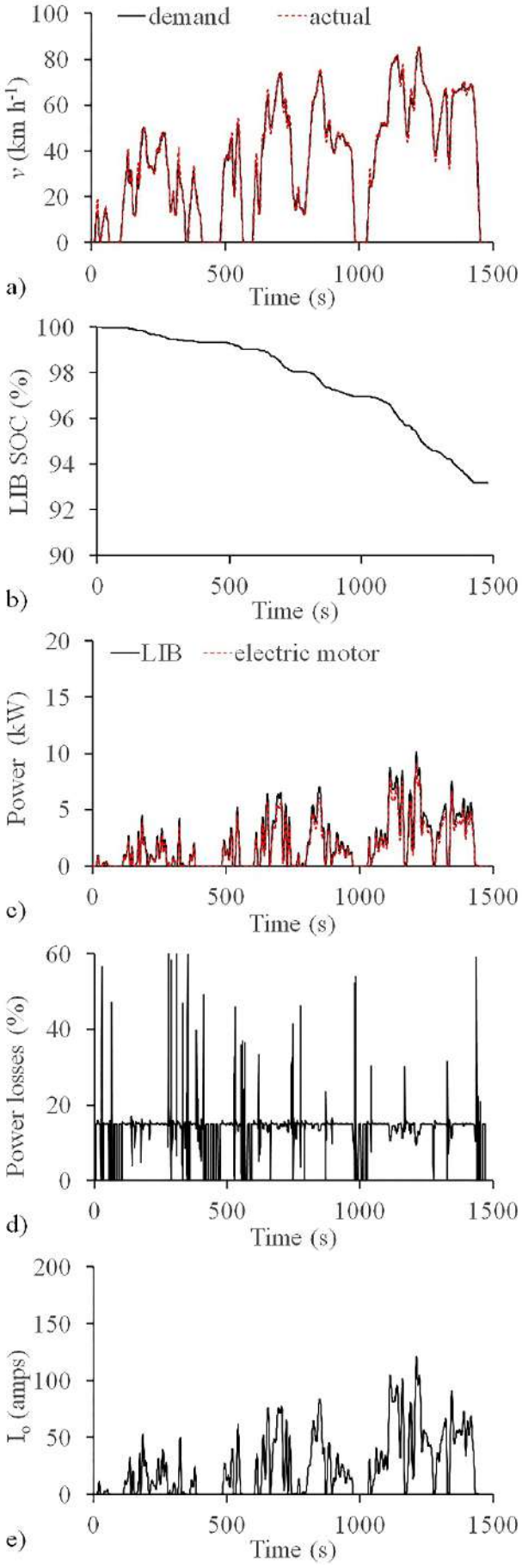

Fig. 8: E-TWV characteristic based on the WLTP class 2

road duty cycle a) vehicle speed b) LIB SOC c) electrical power output d) electrical power losses and e) LIB pack current

Using the results from all road duty cycles in terms of vehicle range per single charge, the estimated well-to-wheel CO_2 emissions were calculated based on Eq. 5 and Table 5 and is shown in Fig. 9. There are small differences in terms of CO_2 emissions for e-TWV in all road duty cycles using coal as the electrical energy source compared to fossil-fuel TVW. This emphasized that the need to have a clean energy source for electric mobility to achieve an efficient system.

Table 5. CO2 emission for the electrical energy generation

CO_2 emission		**Value**
Energy production sources	Coal (g CO_2 MW^{-1} h^{-1})[23]	910000
	Natural gas (g CO_2 MW^{-1} h^{-1})[23]	604000
	Combined cycle (CC) gas turbine (g CO_2 MW^{-1} h^{-1})[24]	407000
% of transmission losses[25]		9.7
% of charging losses at 10 amps rate[26]		6.9

It can be observed that FTP-75 produced the highest well-to-wheel CO_2 emissions for all energy sources, followed by modified ARTEMIS and WLTP class 2. The differences of well-to-wheel CO_2 emission in each of the road duty cycles showed that the importance of controlling the energy demand at the transient response, particularly at stop-start strategies. The source of the energy is also significant to determine the level of well-to-wheel CO_2 emissions. A survey performed by Kana et al.[24] shows that solar power generation has a greater impact on environmental policy. Gima and Yoshitake[27] also indicated that the security of power generation is important for technology sustainability.

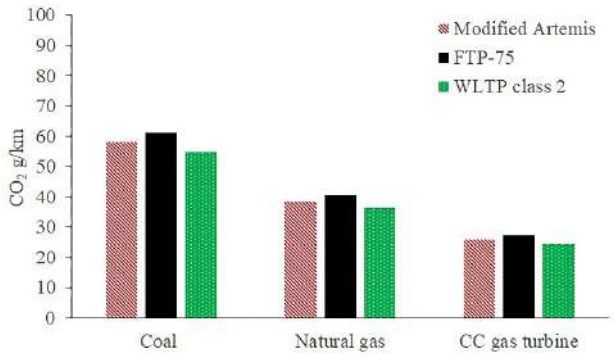

Fig. 9: Well-to-wheel emissions of E-TWV based on different road duty cycles and energy sources.

The E-TWV model was also capable to run in a real-time environment with a standard computational time requirement of < 50 % for control development using hardware-in-the-loop platform[28]. The computational time based on the simulation time and step size was:

- Modified Artemis at 3.7 %
- FTP-75 at 3.5 %
- WLTP class 2 at 2.5 %

4. Conclusions

This study has validated the performance attributes (power and energy interaction) of a high-fidelity E-TWV model for electric motor sizing, controller, and LIB design. The E-TVW performance results revealed a good correlation with a similar product category. The controller block effectively managed the sub-systems interaction with less than 2 % error for transient power demands in different standard road duty cycles. The results also revealed the potential of reducing range anxiety through effective energy management strategies or an appropriate LIB cell architecture (series and parallel) to achieve the desired torque and power. Perhaps, the different trend of energy consumptions in different road duty cycles indicates that more efficient controllers are required to manage the energy flow from the LIB for further optimizing the operating points of electric motor. Passive energy management can also be included such as the design of the E-TWV for lower resistance forces to minimize the chain-drive losses. The differences of well-to-wheel CO_2 emission among the road duty cycles also highlight the importance of controlling the energy demand at the transient response, particularly at stop-start strategies. Nevertheless, the source of electrical energy is imperative to produce low CO_2 well-to-wheel emissions. Carbon-neutral fuels or renewable energies can help vehicle electrification technologies to meet the stringent future emissions directives. The ability of the E-TWV to run in real-time in transient power demands provides the opportunity to develop advanced control strategies in the hardware-in-the-loop platform for system energy management and LIB thermal management.

Acknowledgements

The authors would like to thank Veitis Limited and the School of MAA, Coventry University for providing us with information and support in this research activity.

Nomenclature

P_v	power demand (kW)
A	vehicle frontal area (m^2)
m	vehicle weight (kg)
C_d	coefficient of drag
C_{rr}	tyre rolling resistance
v	vehicle velocity (m s^{-1})
g	gravitational acceleration (m s^{-2})
P_{dc}	direct current power (kW)
V_o	battery pack voltage (V)
I_o	battery pack current (amps)
Δm	weight transfer (kg)
h	height of CoG (m)
l	wheelbase length (m)

K_e	well-to-wheel CO_2 emissions (g km^{-1})
U_e	production CO_2 emission (g CO_2/MWh)
T_e	transmission CO_2 emission (g CO_2/MWh)
C_e	charging CO_2 emission (g CO_2/MWh)

Greek symbols

ε	energy consumption (kW h)
φ	longitudinal acceleration (m s^{-2})
ε_{km}	energy consumption per km (W h km^{-1})
θ	gradeability (°)

References

1) IEA. Tracking Transport 2020. n.d. https://www.iea.org/reports/tracking-transport-2020 (accessed November 10, 2020).
2) N.A. Lestari, "Reduction of CO_2 Emission by Integrated Biomass Gasification-Solid Oxide Fuel Cell Combined with Heat Recovery and in-situ CO_2 Utilization," *Evergreen* **7** *(2)* 209-215 (2020). doi:10.5109/4055220.
3) D. Insights, "Electric vehicles: Setting a course for 2030," n.d. https://www2.deloitte.com/uk/en/insights/focus/future-of-mobility/electric-vehicle-trends-2030.html (accessed November 10, 2020).
4) M. Team, "Global Motorcycles sales fell 21.5% in the first eight months," n.d. https://www.motorcyclesdata.com/2020/09/21/world-motorcycles-market/ (accessed November 10, 2020).
5) "Global Electric Motorcycles Market Research Report," n.d. https://www.marketresearchfuture.com/reports/electric-motorcycles-market-8136 (accessed November 15, 2020).
6) "India considers banning fossil fuel bikes & trikes," n.d. https://www.electrive.com/2019/05/23/india-considers-banning-fossil-fuel-bikes-trikes/ (accessed November 11, 2020).
7) R.M.R.A. Shah, M.A. Qubeissi, A. McGordon, M. Amor-Segan, and P. Jennings, "Micro Gas Turbine Range Extender Performance Analysis Using Varying Intake Temperature," *Automot. Innov.* **3** 356–365 (2020). doi:10.1007/s42154-020-00119-9.
8) J.-H. Wu, C.-W. Wu, C.-T. Lee, and H.-J. Lee, "Green purchase intentions: An exploratory study of the Taiwanese electric motorcycle market," *Journal of Business Research* **68** *(4)* 829-833 (2015). doi:10.1016/j.jbusres.2014.11.036.
9) S. Hardman, A. Jenn, G. Tal, J. Axsen, G. Beard, N. Daina, E. Figenbaum, N. Jakobsson, P. Jochem, N. Kinnear, P. Plötz, J. Pontes, N. Refa, F. Sprei, T. Turrentine, and B. Witkamp, "A review of consumer preferences of and interactions with electric vehicle charging infrastructure," *Transportation Research Part D: Transport and Environment*. **62** 508-523 (2018). doi:10.1016/j.trd.2018.04.002.
10) S.Z. Rajper, and J. Albrecht, "Prospects of Electric Vehicles in the Developing Countries: A Literature Review," *Sustainability* **12** *(15)* 1906 (2020). doi: 10.3390/su12051906.
11) S. M. Ali, and A. Chakraborty, "Performance Study of Adsorption Cooling Cycle for Automotive Air-conditioning," *Evergreen* **2** *(1)* 12-22 (2015). doi:10.5109/1500423
12) A. Guizani, M. Hammadi, J.-Y. Choley, T. Soriano, M.S. Abbes, and M. Haddar, "Electric vehicle design, modelling and optimization," *Mechanics & Industry* 2016. **17** 405 (2016). doi:10.1051/meca/2015095.
13) R.A. Hanifah, S.F. Toha, N.H.H.M. Hanif, and N.A. Kamisan, "Electric Motorcycle Modeling for Speed Tracking and Range Travelled Estimation," *IEEE Access* **7** 26821-26829 (2019). doi: 10.1109/ACCESS.2019.2900443.
14) V. Nguyen, H. Pyung, and T. Huynh, "Computational analysis on Hybrid Electric Motorcycle with front wheel electric motor using Lithium Ion battery," *International Conference on System Science and Engineering* 335-359 (2017). doi: 10.1109/ICSSE.2017.8030896.
15) P.-T. Chen, D.-J. Shen, C.-J. Yang, and K.D. Huang, "Development of a Hybrid Electric Motorcycle that Accords Energy Efficiency and Controllability via an Inverse Differential Gear and Power Mode Switching Control," *Appl. Sci.* **9** *(1787)* (2019). doi:10.3390/app9091787.
16) M. Marinov, V. Valchev, R. Stoyanov, and P. Andreev, "An Approach to the Electrical Sizing of The Electric Motorcycle Drive," *20th International Symposium on Electrical Apparatus and Technologies (SIELA)* 1-4 (2018). doi: 10.1109/SIELA.2018.8447065.
17) R.E. Dorey, and E.J. Martin, "Vehicle Driveability - The Development of an Objective Methodology," *SAE Technical Paper* 01-1326 (2000). doi:10.4271/2000-01-1326.
18) "CO2 emissions from Motorcycles: Learning's from cars," n.d. https://www.lowcvp.org.uk/assets/presentations/MCI%20-%20Greg%20Archer.pdf (accessed November 14, 2020).
19) A. Houidi, A. Khadr, and L. Romdhane, "Dynamic modeling and handling study of a two-wheeled vehicle on a curved track," *Mechanics & Industry* **18** 409 (2017). doi:10.1051/meca/2017005.
20) T. Tsubota, A. Kitajou, and S. Okada, "O3-type Na (Fe_1/3Mn_1/3Co_1/3) O_2 as a Cathode Material with High Rate and Good Charge-Discharge Cycle Performance for Sodium-Ion Batteries," *Evergreen* **6** *(4)* 275-279 (2019). doi:10.5109/2547348.
21) B. Xie, A. Kitajou, S. Okada, W. Kobayashi, M. Okada, and T. Takahara, "Cathode Properties of

Na_3MPO_4CO_3 (M= Co/Ni) Prepared by a Hydrothermal Method for Na-ion Batteries," *Evergreen* **6** *(4)* 262-266 (2019). doi:10.5109/2547345.

22) M. Spöttle, K. Jörling, M. Schimmel, M. Staats, L. Grizzel, L. Jerram, W. Drier, and J. Gartner, "Research for TRAN Committee - Charging infrastructure for electric road vehicles," *European Parliament: Brussels* n.d. https://op.europa.eu/en/publication-detail/-/publication/3218a76f-79b8-11e8-ac6a-01aa75ed71a1/language-en (accessed November 16, 2020).
23) C. Murphy, and C.Cunliff, "Environment Baseline, Volume 1: Greenhouse Gas Emissions from the U.S. Power Sector. 2016," *Office of Energy Policy and Systems Analysis U.S. Department of Energy* n.d. https://www.energy.gov/sites/prod/files/2017/01/f34/Environment%20Baseline%20Vol.%201--Greenhouse%20Gas%20Emissions%20from%20the%20U.S.%20Power%20Sector.pdf (accessed November 20, 2020).
24) "Transmission Losses," *nationalgridESO* n.d. https://www.nationalgrideso.com/document/144711/download (accessed November 20, 2020).
25) E. Apostolaki-Iosifidou, P. Codani, and W. Kempton, "Measurement of power loss during electric vehicle charging and discharging," *Energy* **127** 730-742 (2017). doi:10.1016/j.energy.2017.03.015.
26) K. Moroga, A. Nagata, Y. Kuriyama, T. Kobayashi, and K. Hasegawa, "State of implementation of environmental and energy policies adopted by the regional governments in Japan," *Evergreen* **2** *(2)* 14-23 (2015). doi:10.5109/1544080.
27) H. Gima, and T. Yoshitake, "A Comparative Study of Energy Security in Okinawa Prefecture and the State of Hawaii," *Evergreen* **3** *(2)* 36-44 (2016). doi:10.5109/1800870.
28) R. M. B. R. A. Shah, R.P. Jones, C. Cheng, G. Dhadyalla, J. Pawar, and S. Biggs, "A low fidelity nonlinear model of 4WD torsional stiffness at tip-in/tip-out," *FISITA 2010 World Automotive Congress* 1-8 (2010).